Tibaldi *et al.*
Journal of Occupational Medicine and Toxicology (2024) 19:45
https://doi.org/10.1186/s12995-024-00434-5

Journal of Occupational Medicine and Toxicology

RESEARCH

Open Access

Pathological characterization of lung fibrosis in Sprague–Dawley rats treated with fluoro-edenite fibres by intrapleural injection

Eva Tibaldi[1†], Federica Gnudi[1†], Daniele Mandrioli[1*†], Caterina Bruno[2†], Amerigo Zona[2], Lucia Fazzo[2] and Pietro Comba[2†]

Abstract

Background An increased incidence of pleural mesotheliomas in Biancavilla (Italy) was attributed to the environmental exposure to fluoro-edenite (FE). Results from the Ramazzini Institute (RI) in vivo long-term study confirmed the evidence that exposure to FE fibres is correlated with an increase of malignant pleural mesotheliomas in Sprague–Dawley rats. Recently asbestosis-like features were substantiated in Biancavilla residents without known occupational exposures. Aim of this work was to establish whether FE induce lung fibrosis with a pathogenetic mechanism similar to other asbestiform fibres.

Methods Original slides from the RI study were systematically re-examined to characterize the FE-induced lesions. Quantitative analysis of lung fibrosis was assessed following the Ashcroft method. Immunohistochemical analysis of protein involved in fibrotic responses and histochemical staining for FE-fibres identification were performed.

Results Like asbestos, FE caused fibrotic lesions, pleural plaques or nodules and mesotheliomas. A significant increase of lung fibrosis ($p < 0.001$) was observed in the FE-treated groups compared to untreated controls. In the fibrotic responses to FE, vimentin was the most expressed protein, followed by collagen-I and alpha-SMA. Finally, ferruginous bodies, characterized by iron deposits and ferritin expression, were observed in FE-induced lesions.

Conclusions This study confirmed that FE exposure promotes the onset of fibrotic lesions at pleural level, as fibrous plaques or nodules and fibrosis, through a mechanism similar to other form of asbestos. These results combined with epidemiological study reported in Biancavilla residents, corroborate the need to promote health and epidemiological surveillance plans of respiratory diseases in population living in FE contaminated sites.

Keywords Fluoro-Edenite, Mesothelioma, Fibrosis, Ashcroft quantification, Immunohistochemistry

†Eva Tibaldi, Federica Gnudi and Daniele Mandrioli are co-first authors.

†Caterina Bruno and Pietro Comba are retired.

*Correspondence:
Daniele Mandrioli
mandriolid@ramazzini.it
[1]Ramazzini Institute, Cesare Maltoni Cancer Research Center, Via Saliceto 3, Bologna, Bentivoglio 40010, Italy
[2]Enviroment and Health Department, Istituto Superiore Sanità (ISS), Roma, Italy.

Background

The fluoro-edenite case stemmed from a national survey on mortality by pleural mesothelioma in Italy. It found an excess of mesothelioma cases at Biancavilla, a town of nearly 23,000 inhabitants perched on the south-west side of Mount Etna. Between 1988 and 1992 four cases of pleural mesothelioma were reported there [1, 2]. From the statistics calculated on the basis of the Sicilian population the expected cases at Biancavilla over the same period were 0.9 (SMR 417; 95% CI 142–954) [3]. This preliminary finding led to an epidemiological study performed by the Italian National Health Institute (ISS) which unearthed a total of 17 cases of pleural mesothelioma (10 men and 7 women) among the town inhabitants from 1980 to 1997 [2, 4, 5]. The study verified that asbestos exposure might have been the cause in two of these cases; in other 5 such exposure could not be entirely ruled out; the remaining 10 could reasonably be ascribed to general environmental exposure. In a pilot study of Biancavilla inhabitants, some of whom were special hospital cases with a flare-up of chronic symptoms of obstructive pulmonary disease, 6 out of 12 patients (2 men and 4 women) had fluoro-edenite fibres in their sputum [6]. Since the data on occupational exposure did not show that the mesothelioma group might be correlated to asbestos exposure, it was inferred that the general environment might have been the cause. Thus, a mineralogical study was started in the area of Biancavilla, where incohesive volcanic material (pyroclastic deposits) had been largely used in local building industry (walls, render, cement mortar), as well as to pave roads, squares and other areas [2, 7]. The quarry was mined at least since the 1950s, with a production peak in the 1960s-1970s [8, 9]. This area is made up of domes and dikes associated with a fine-grained material in which unknown amphibolic fibres with fluoro-edenitic composition were found and that was initially classified as an intermediate phase between tremolite and actinolite [10–12]. Fluoro-edenite (FE) exists as millimetre-scale crystals, as well as loose asbestiform (fibrous) fibres in rock cavities. The United States National Institute for Occupational Safety and Health (NIOSH) described the morphology of these elongated minerals as acicular, prismatic or asbestiform [13]. FE is generally associated with potassium feldspars and plagioclase, quartz, clino- and orthopyroxenes, fluoro-apatite, ilmenite, and abundant haematite [14]. The Commission on New Minerals and Mineral Names of the International Mineralogical Association (IMA, code 2000–049) entered a new end-member of the amphibole calcic group of the edenites, the fluoro-edenite series, due to its high content in fluorine and sodium, especially compared to tremolite and actinolite fibres [10, 14].

In the Ramazzini Institute (RI) laboratory, as part of a cancer research program designed in the late 1970s to identify industrial and environmental carcinogens, a large, integrated, long-term, an in vivo project was begun on fibrous and/or corpuscular matter. Among the studied materials there were asbestos and many other kinds of diverse fibre, various kinds of natural zeolites (sedimentary and hydrothermal) including erionite, various synthetic zeolites and other organic compounds, natural and artificial solids like silica, alumina, talc, kaolin, synthetic or artificial mineral fibres, propylene fibre, etc. The aim of the RI project was not only to verify the carcinogenicity of various materials, but also to provide information on the relative carcinogenic potential. To that end, all compounds were tested in the same experimental conditions. In the two-year study on FE, the onset of pleural and peritoneal mesothelioma in Sprague–Dawley (SD) rats from our own breeding facility only 36 weeks after injection with FE fibres was observed. In 2004 the RI published the preliminary results to sensitize the population and the authorities about the probable risk that Biancavilla's people were taking. The RI also tried to set in motion urgent environmental-health controls, given that our preliminary results had brought to light several cases of mesothelioma in treated animals [15]. When the final results came out in 2011, [16] from the epidemiological evidence and these experimental results, the International Agency for Research on Cancer (IARC) classified fluoro-edenite as carcinogen to humans (Group 1) [12].

Several detailed mortality and morbidity studies were produced from 2004 through 2011 by the Epidemiological Observatory of Sicily. In addition to pleural mesothelioma, the only neoplastic disease in excess, an excess mortality and hospitalization was estimated from non-malignant respiratory diseases, namely from pneumoconiosis, thus corroborating the notion of the occurrence of environmental lung fibrosis [17]. The health profile of the Biancavilla community, showed similarities with the corresponding health profile of other populations characterized by environmental asbestos exposure due to residence in contaminated areas [18].

Recently, the characteristics of the lung damage residents in Biancavilla hospitalized with pneumoconiosis or asbestosis diagnoses were investigated and asbestos-like features were found in some Biancavilla residents without known occupational exposure to asbestos; experimental studies were recommended by the authors [19].

The aim of this work was to establish whether and how FE-fibres may promote lung fibrosis like other asbestos-fibres.

Methods

Sample selection from RI long-term experiment on fibrous FE (BT2117)

In the RI long-term study on FE effects, fibrous FE, supplied by Dr. Gianfagna (Earth Sciences Department, Sapienza, Università di Roma), was administered to groups of 80 Sprague–Dawley (SD) rats (40 males and 40 females) by intrapleural injection, once-off, at the dose of 25 mg suspended in 1 cc of water. A group of 80 rats (40 males and 40 females) was injected with water as controls. Animals were kept under observation until their natural death. The experiment was conducted following the principles of Good Laboratory Practice (GLP), with the RI Standard Operative Procedures and with the Italian Government Guidelines for use of experimental animals (Governo Italiano, D.Lgs 116/1992) [15, 16].

Alcohol fixed-Paraffin-embedded samples of SD rat lung from the long-term carcinogenicity study on fibrous FE administered by intrapleural injection were retrieved from the RI Biobank. For each paraffin block, 6 serial sections were obtained using a rotating microtome (Leica Biosystem, Wetzlar, Germany) and collected in polylysine-coated slices for histochemical and immunohistochemical analysis.

Morphological characterization of pathological lesions

Original slides stained with Haematoxylin and Eosin (HE) were systematically examined blind and independently by two different pathologists using the same morphological criteria. The morphological assessment considered anatomic architectural alterations in lung and, if an abnormal population was detected, the pattern and the cell size and nuclear characteristics were determined. When the review found lack of concordance between the two pathologists, a third senior pathologist performed an additional examination to establish the final diagnosis.

Semi-quantitative assessment of lung fibrosis

Paraffin-embedded lung tissue sections were deparaffinised in xylene and hydrated through a series of alcohols to water. Sections were stained with Masson's Trichrome Goldner variant (Bioptica, Milano). Quantitative assessment of lung fibrosis was performed using the Ashcroft score method [20, 21]. Stained slides were systematically scanned with a NIKON Eclipse Ni optical microscope using a 10X objective. Forty images were randomly selected using NIS Element Advanced Research software. These images were analyzed by two different pathologists and lung fibrosis was scored according to a predetermined scale of severity from 0 to 8. For each sample up to 40 fields were evaluated and each field was assigned a score according to the aforementioned predetermined scale. For each sample, the mean and median of the scores was calculated as an indicator of the measurements. The average of mean and median scores per animal were statistically analyzed and described separately by sex and by treatment (control vs treated). Differences in scores between treated and control group was examined using a Two-sample Wilcoxon rank-sum (Mann–Whitney) test [22]. The software used for the analysis was Stata 18.

In parallel, a panel of three different antibodies were used for the evaluation of lung fibrosis by immunohistochemistry (IHC). Alpha-smooth muscle actin (alpha-SMA, #MA1-06110, Thermo Fisher Scientific, Waltham, Massachusetts, USA), collagen type I (COL1, #NB600408, Novus Biological, Centennial, Colorado, USA) and vimentin (#sc-371717, Santa Cruz Biotechnologies, Dallas, Texas, USA).

These proteins are widely used as markers that drive fibrosis with different mechanisms of action. Alpha-SMA is a biomarker for myofibroblast differentiation, COL1 involved in the activation of collagen receptors influencing cell behaviour during progressive fibrosis, and vimentin is a key regulator of fibrosis and it is strongly expressed in mesenchymal cells.

The analysis was performed on a total of 39 samples that were considered representative of the fibrotic lesions of interest, from the pool of the treated female and male groups. In particular 8 cases of mesothelioma (3 females and 5 males), 6 cases of fibrous plaque or nodules (3 females and 3 males) and 25 cases of fibrosis (14 females and 11 males) were analysed. Paraffin-embedded lung tissue sections were deparaffinised in xylene and hydrated through a series of alcohols to water. Non-specific background was blocked using 0.3% hydrogen peroxide and serum-free protein block (Biocare Medical, Pacheco, CA, USA). After blocking, slides were incubated with primary antibody against alpha-SMA (dilution 1:300 for 1 h at room temperature), or COL1 (dilution 1:200 overnight at 4 °C), or vimentin (dilution 1:100 for 1 h at room temperature). Positive and negative controls (omission of the primary antibody and of IgG-matched serum) were included. Anti-mouse or anti-rabbit HRP polymer detection kit (Vector Laboratories, Burlingame, CA, USA) was added to the sections and incubated for 30 min at room temperature. The entire antibody-enzyme complex was made visible by reaction with diaminobenzidine (DAB) until adequate colour development was observed (DakoCytomation, Santa Clara, CA, USA). Finally, sections were rinsed in distilled water, counterstained with haematoxylin, dehydrated, and cleared in xylene. Cover slips and mountant were applied for optical microscopy analysis. Slides were systematically examined blind, without prior knowledge of the groups, and independently by two different pathologists. Wherever agreement was

not reached, a third senior pathologist established the final diagnosis and score. Criteria for sufficient staining were antibody binding specificity, tissue morphology and overall staining quality. Grading of the specific immunoreactivity was based on a six-point scale with – (negative); -/+ (very rare positivity); ± (scattered positivity); + (weak diffuse positivity); + + (diffuse positivity) and + + + (strong positivity).

Histochemical and Immunohistochemical evaluation of iron deposits in lungs

Paraffin-embedded lung tissue sections were deparaffinised in xylene and hydrated through a series of alcohols to water. Sections were stained with Perls' staining (Bioptica, Milano). Samples were analysed using a Leica Microscope (Leica Microsystems GmbH, Germany).

Ferritin expression was evaluated by IHC and immunofluorescence (IF). IHC was performed following the protocol used for alpha-SMA, COL1 and vimentin staining. Slides were incubated with primary antibody against Ferritin (#sc-376594, Santa Cruz Biotechnologies, Dallas, Texas, USA) at a dilution of 1:150 at 4 °C overnight.

For IHC, anti-mouse HRP polymer detection kit (Vector Laboratories, Burlingame, CA, USA) was added to the sections and incubated for 30 min at room temperature. The entire antibody-enzyme complex was made visible by DAB (DakoCytomation, Santa Clara, CA, USA).

For IF, DyLight® 549 Anti-mouse IgG (H + L) (Vector Laboratories, Burlingame, CA, USA) were used as secondary antibody. Sections were rinsed in distilled water and once dried (approximately 3 min), three drops of VECTASHIELD® Antifade Mounting Medium with DAPI (Vector Laboratories, Burlingame, CA, USA) were added. Slides were then covered with a coverslip and were kept in the dark for 24 h at 4 °C before imaging. Fluorescence was analyzed microscopically with a photomicroscope Nikon Ni-E (Nikon, Japan) equipped with epifluorescence.

Results

Morphological characterization of pathological lesions

In the FE-treated group, neoplastic and non-neoplastic lesions being pleural mesotheliomas (13/80, 16.3%), pleural plaques or nodules (6/80, 7.5%), and pleural fibrosis (51/80, 63.8%) were diagnosed (Tables 1 and 2).

Among the 13 cases of mesotheliomas, 6 were observed in males and 7 in females. In males, the most prevalent histotype was the epithelioid one.

Their histological features included tubule-papillary, trabecular, or adenomatoid architectural patterns,

Table 1 Incidence of pleural mesotheliomas and histotype

Group	Treatment	Dose (mg/cc H_2O)	Route of administration	Animals		Malignant Mesothelioma		Histotype		
				Sex	No	No	%	Epitheliod	Biphasic (mixed)	Sarcomatoid
I	Fibrous FE	25	Intrapleural Injection	M	40	6	15.0	3 (50.0%)	2 (33.3%)	1 (16.7%)
				F	40	7	17.5	0 (0.0%)	4 (57.1%)	3 (42.9%)
				M + F	80	13	16.3			
II	-	0	Injection with water	M	40	0	-			
		(control)		F	40	0	-			
				M + F	80	0	-			

Table 2 Histomorphological evaluation of lung samples in the FFE-treated SD rat study. Incidence of preneoplastic pleural nodules or plaques and fibrosis

Group	Treatment	Dose (mg/cc H_2O)	Route of administration	Animals		Fibrous plaque or nodule		Fibrosis	
				Sex	No	No	%	No	%
I	Fibrous FE	25	Intrapleural Injection	M	40	3	7.5	27	67.5
				F	40	3	7.5	24	60.0
				M + F	80	6	7.5	51	63.8
II	-	0	Injection with water	M	40	0	-	0	-
		(control)		F	40	0	-	0	-
				M + F	80	0	-	0	-

lympho-histiocytoid cytological features, or myxoid stroma [16, 23]. Two cases out of the six males were identified as biphasic (or mixed) subtype showing both epithelioid and sarcomatous components. Finally, only one case was identified as sarcomatous/fibrous subtype, composed of elongated/spindle cells arranged in solid sheets or within a fibrous stroma. In females the biphasic (or mixed) subtype was the most prevalent (4/7 cases), followed by the sarcomatous/fibrous one (3/7 cases).

Finally, all of the non-neoplastic lesions examined were accompanied by reactive inflammation affecting pleura and lung parenchyma. Moreover, fibrosis was associated with the presence of FE-fibres. No lesions were observed in untreated controls.

Semi-quantitative assessment of lung fibrosis

Forty fields per animal were analysed and scored using an Ashcroft scale. The distribution of frequency of the scores for each field is summarized in Fig. 1 and Table 3. For each animal we then calculated a mean and a median Ashcroft score, and these summary measures were used to calculate the mean Ashcroft scores and SD by sex and treatment. These results are showed in Table 4.

Table 3 reports the absolute number of times each score was used and the percentage frequency. A descriptive analysis of all evaluated fields shows how, both in females and males, more than 2/3 of the scores in control group were 0, while they drop to around 40% in treated animals. The scores used for mild fibrosis (scores 1, 2 and 3) represent 23 to 27% in control animals, while they range from 37 to 43% in treated animals. Conversely, scores < 3, signaling moderate to strong fibrosis, are used more often (28

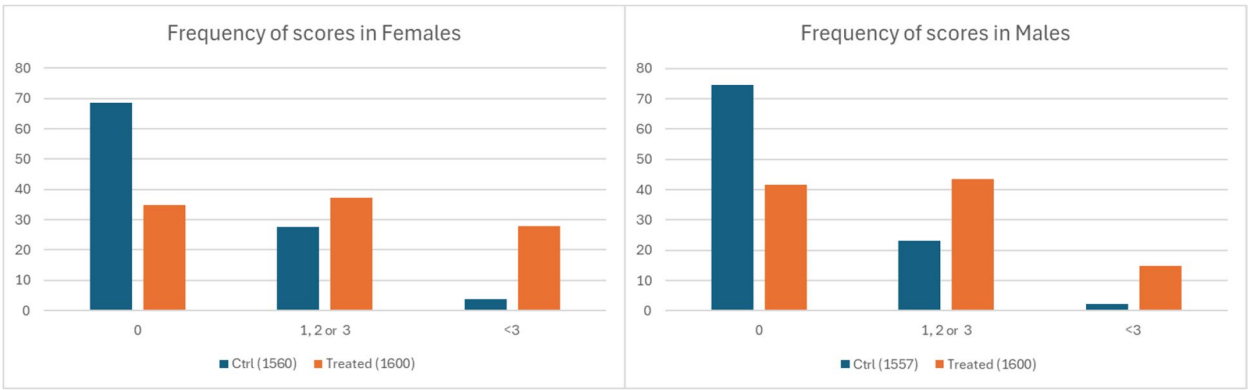

Fig. 1 Frequency of Ashcroft scores assigned in each field by sex and treatment

Table 3 Frequency of Ashcroft Scores by sex and group (number of fields and percentage)

Scores	Females				Males			
	Controls (1560)	%	Treated (1600)	%	Controls (1557)	%	Treated (1600)	%
0	1071	68.65	556	34.75	1162	74.63	665	41.56
1, 2 or 3	430	27.56	598	37.37	359	23.06	697	43.56
< 3	59	3.78	446	27.87	36	2.31	238	14.87

Table 4 Average Ashcroft scores by sex and group of the mean and median Ashcroft scores per animal

Group	Treatment	Dose (mg/cc H_2O)	Route of administration	Animals		Ashcroft scores Mean		Ashcroft scores Median	
				Sex	No	Mean	SD	Mean	SD
I	Fibrous FE	25	Intrapleural Injection	M	40	1.58*	0.87	1.05*	1.22
				F	40	2.28*	0.95	1.95*	1.59
II	-	0	Injection with water	M	39	0.47	0.24	0.01	0.08
		(control)		F	39	0.60	0.20	0.01	0.08

* Statistically significant with Mann–Whitney test ($P < 0.0001$)

and 15% for females and males, respectively) for treated animals, while they represent a residual 4 and 2% for the control animals. These results can be visualized in Fig. 1.

Control animals

In females one animal presented an atypical renal mesenchymal tumour metastasis in the lungs, influencing the level of inflammation and fibrosis, and was therefore considered an outlier and excluded from the analysis. This resulted in 39 lung samples from female untreated animals, for a total of 1560 fields analysed. The mean Ashcroft score per animal was always < 1, while the median per animal was 0 in all cases but one (0.5). The mean per group of the mean Ashcroft score per animal was 0.60 (S.D. 0.20) and the mean value of the median was 0.01 (SD 0.08) (see Table 4 and supplementary material).

In males, again one animal was considered an outlier due to his fibro-histiocytic sarcoma of the lungs and not included in the analysis; furthermore, three more observations from another animal were not available due to insufficient sampling material, leading to a total of 1557 observed fields. The mean Ashcroft score per animal was < 1 in all cases but one (1.225), similarly the median per animal was 0 in all cases but one (0.5). The mean per group of the mean Ashcroft score per animal was 0.47 (SD 0.24) and the mean value of the median was 0.01 (SD 0.08) (see Table 4 and supplementary material).

In female and male controls, fibrosis was limited to a few perivascular, peribronchial or subpleural areas. Sporadic occurrence of minimal fibrotic lesions was compatible with the age of rats. The difference in the average Ashcroft score between the groups, 0.60 in females and 0.47 in males, could be attributable to the mean age at death (94.1 weeks for males and 101.9 weeks for females) (see supplementary material).

Fibrous FE-treated SD rats

Forty fields per animal were analysed and scored using an Ashcroft scale for a total of 1600 scores for treated males and females.

In female FE-treated group we observed a higher variability in the mean Ashcroft score per animal: 19 had mild fibrosis with an average score between 1 and 2 (47.5%); 17 had moderate fibrosis with an average score between 2.1 and 3 (42.5%); finally, 4 cases, including 3 rats with diagnosis of mesothelioma, had severe fibrosis with an average score > 3 (10%). In animals bearing mesothelioma, 2 cases had a mean score between 1 and 2; 2 cases > 2; and 3 cases > 4. In animals showing pleural plaques, 2 cases had a mean score > 2 and 1 case had a score between 1 and 2. Similarly, the median scores per animal were more heterogeneous, ranging from 0 to 7.5 (see supplementary material). The mean per group of the mean Ashcroft score per animal was 2.28 (SD 0.95), three times higher than control, and mean value of the median was 1.95 (SD 1.59).

In male FE-treated group, we observed a higher variability in the mean Ashcroft score per animal: 35 had mild fibrosis with an average score between 1 and 2 (87.5%), 3 had moderate fibrosis with an average score between 2.1 and 3 (7.5%) and 2 had severe fibrosis with an average score > 3 (5%). In animals bearing mesothelioma, 4 had an average score between 1 and 2, and 2 had an average score > 3. In animals showing pleural plaques, mean Ashcroft score did not exceed value of 1. Similarly, the median scores per animal were more heterogeneous, ranging from 0 to 7(see supplementary material). The mean per group of the mean Ashcroft score per animal was 1.58 (SD 0.87), three times higher than control, and mean value of the median was 1.05 (SD 1.22).

The statistical analysis of the group mean of the mean and median Ashcroft scores showed a statistically significant increase of fibrosis ($p < 0.0001$) in both male and female FE-treated animals compared to controls (Table 4).

In 24 out of 40 FE-treated female rats (60%) and in 27 out of 40 FE-treated male rats (67.5%), fibrosis was diagnosed at pleural and subpleural level. In animals with the highest score, fibrosis was also present into the alveolar parenchyma and not only in peribronchial or perivascular areas.

Fibrosis induced by FE-treatment was frequently associated with inflammatory reaction characterized by macrophages, granulocytes, and multinucleated giant cells, mainly found in the pleura. Mesothelioma histotypes differed in the degree of fibrosis: the sarcomatous histotype had very high score due to the high presence of collagen fibres compared to biphasic and epithelioid ones. For this reason, not all mesotheliomas achieved similar scores. Other fibrotic lesions observed in FE-treated groups were fibrous plaques, nodules, and pleural fibrosis. In both mesotheliomas and pleural plaques, the extension of fibrosis frequently affected the diaphragm.

Immunohistochemical (IHC) characterization of lung fibrosis

Alpha-SMA, COL1-A and vimentin, showed variable grades of positivity in mesotheliomas, while no marker was expressed in untreated controls. Vimentin was the most expressed marker, showing positivity also in mild lesions. Alpha-SMA was found to be the least expressed marker overall, but still positive in mesotheliomas and pleural plaques. Collagen type I was generally more expressed than alpha-SMA showing strong positivity in severe lesions and weak positivity in pleural fibrosis. The overall results underlined that mesotheliomas were

characterized by high degrees of fibrosis. In fibrotic plaque or nodule and in fibrosis with fibre deposits, the positive staining for vimentin underlined mesenchymal cell activation and collagen production (Fig. 1). In mild lesions, a variable grade of positivity was observed only for vimentin, showing that the first stage of fibrosis development is the activation of mesenchymal cells.

Perls' staining for the identification of iron deposits in lungs

Perls' staining was performed to evaluate the presence of FE fibres and their chemical composition by the indirect staining of iron deposits in lung tissue samples and to understand the mechanisms of interaction between fibres and tissues.

In 27 out of 39 stained lung samples (14 females and 13 males, 69.2%), the presence of ferruginous bodies near or engulfing FE fibres was observed (Fig. 2). Of the remaining 12 cases, fibres were not present in 6 cases (3 females and 3 males, 15.4%). In the remaining 6 cases (3 females and 3 males, 15.4%), fibres were detected but ferruginous bodies were not found around them. Most cases with fibre deposits showed a concomitant formation of ferruginous bodies of different shapes and sizes covering either the entire fibre or part of it. In mesotheliomas iron deposits were observed in intercellular or intracellular spaces (Fig. 3).

Immunohistochemical and immunofluorescence analysis of ferritin in lungs

IHC analysis of ferritin and Perls' staining showed comparable results. In 27 cases (69.2%), ferruginous bodies

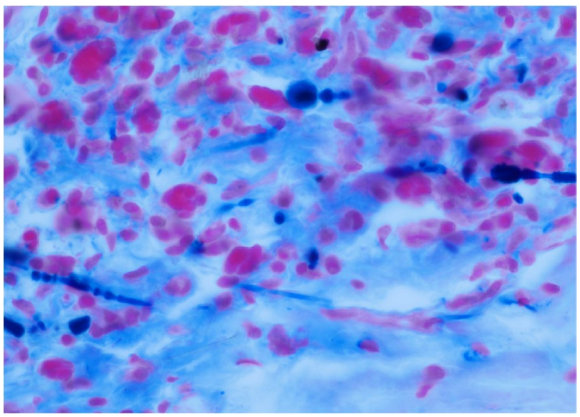

Fig. 3 Case No. 125 (F) Fibrosis with fiber deposits. This image shows the formation of deep blue ferruginous/asbestiform bodies around the fibers. These formations have different shapes: segmented, rounded or needle-like. (PERLS stain, Magnification 40X)

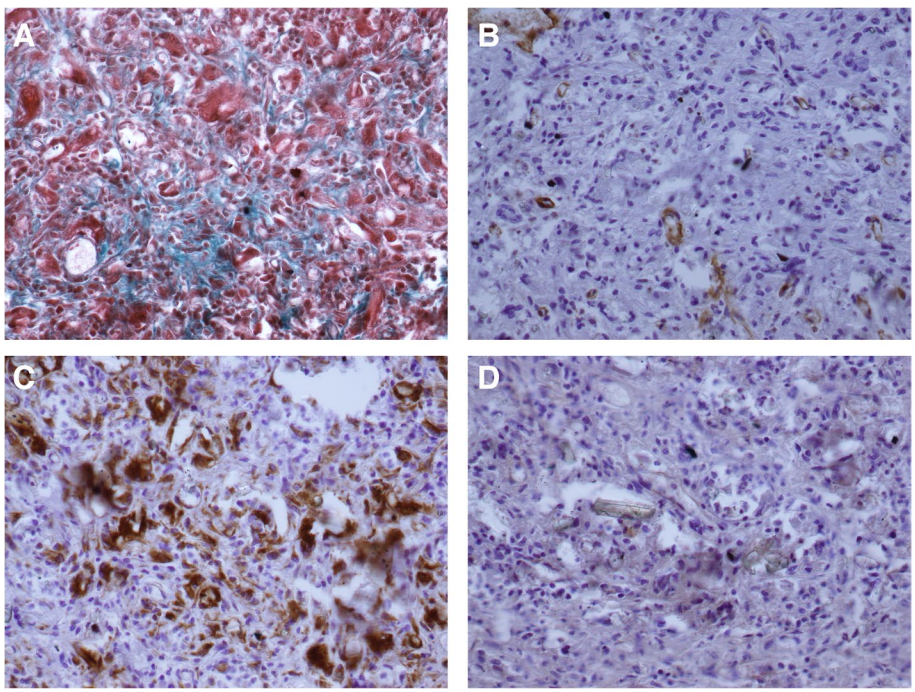

Fig. 2 Case No. 101 Pleural fibrosis with deposits of fibers. A localized fibrosis was observed within a pleural plaque, in which deposits of fibrous FE are visible. Fibrosis is stained in green by Masson's trichrome (**A**). The IHC markers showed different expression: Alpha-SMA is poorly expressed and localized around the vessels (**B**); Vimentin is strongly expressed (**C**); COL-1A is weakly expressed in the area containing fiber deposits (**D**) (Magnification 40X)

showed positivity for both ferritin and Perls' staining. In 6 cases (15.4%), fibres were not observed, and both the staining were negative. In the remaining 6 cases (15.4%), fibres were observed, but no ferruginous bodies or iron deposits were found. Fibrous plaques and fibrosis with fibre deposits showed strong positivity for ferritin around fibres and in extracellular matrix. In mesotheliomas, ferritin expression was lower than in non-neoplastic lesions. In spindle cell mesothelioma, ferritin deposits were observed within the tumour and among the neoplastic cells. In fibrosis, in which no fibres or iron deposits were found, the expression of ferritin was absent. Analysis of ferritin expression was also performed by IF, with ferritin highlighted in red while nuclei in blue.

Discussion

Fibrotic responses to amphibolic fibrous FE were evaluated by a systematic quantitative analysis of SD rat lung samples from the RI long-term experiment. Pathological lesions induced by fibrous FE exposure were re-evaluated. Results showed an increase of mesotheliomas, fibrous plaques or nodules and pleural fibrosis, demonstrating that FE has not only carcinogenic effect, but it is able to induce fibrotic reaction in pleura. Fibrous plaques or nodules were observed in 7.5% of FE-treated SD rats, while fibrosis was observed in 60% of female and 67.5% of male FE-treated SD rats. No lesions were diagnosed in control groups. Then, FE-induced lung fibrosis was quantitatively evaluated by the Ashcroft score method [20]. Results showed that exposure to FE led to a statistically significant increase of both incidence ($p < 0.001$) and degree (> 3 times) of fibrosis in rats compared to controls. Varying degree of fibrosis were also observed in mesotheliomas depending on histotype. In fact, the sarcomatoid mesotheliomas showed higher degree of fibrosis than the epithelial one. Plaques or fibrosis were mainly located at pleural level. Finally, FE-treated rats with fibrotic lesions showed needle-like fibres around and into the lesions. Intrapleural injection is a reference model for long-term carcinogenicity studies of fluoro-edenite and other asbestiform fibers, allowing to elucidate the interplay between fibrogenic mechanisms and cancer at pleural and interstitial level of the lung parenchima. However further inhalation studies might elucidate how other fibrogenic mechanism might play a role in the airways.

IHC analysis of Vimentin, Collagen I and Alpha SMA was performed to further investigate the mechanism of fibrosis development induced by FE exposure. In mesotheliomas, all the proteins showed variable degree of positivity. Vimentin expression, marker of mesenchymal cell origin, is associated with enhanced cell motility, adhesion to the extracellular matrix and collagen deposition. Indeed, the importance of vimentin is now widely recognized in cellular functions ranging from motility to signal transduction [24, 25]. Vimentin has a role in the stabilization of collagen mRNAs that may contribute to the high level of collagen expression by mesenchymal cells [26].On the other hand, alpha-SMA is expressed during transition from fibroblast to myofibroblast, which is is a well-known cellular hallmark of the pathological state of tissues [27].

In our study, vimentin was the most expressed protein even in mild lesions, underlying that mesenchymal cell activation probably occurs during the first stage of fibrosis development. In plaques and fibrosis with FE deposits, vimentin, and collagen I were strong positive. On the other hand, alpha-SMA was weak, suggesting that myofibroblast-like cell activation occurs later than mesenchymal cells activation and collagen production. Here, the degree of fibrosis was higher than in mesotheliomas.

Like asbestos, FE is not only a powerful carcinogen inducing malignant mesotheliomas, but it is also able to cause pleural plaque formation and fibrosis. Although the toxicity of these fibres is certain, the pathogenetic mechanisms and factors that may trigger to pulmonary toxicity and neoplastic transformation are not yet fully understood.

All asbestos fibres cause oxidative stress to the lung by forming free radicals. This process is also linked to the presence of transition metals [28]. The macrophage response to fibre-induced oxidative stress results to reduce free iron to make it less available to the fibre and convert it into the less toxic protein-bound iron. The presence of iron in the fibres (which can contain up to 30% Fe of their weight), their intrinsic ability to attract it from the surrounding environment and the series of cellular reactions that attempt to re-establish a balance in iron metabolism appear to be key factors for the formation of "ferruginous or asbestiform bodies" in the lung, hallmarks of exposure to asbestiform fibres [29]. The formation of an "asbestiform body" is a phenomenon involving the deposition of endogenous iron, iron-containing proteins, such as ferritin, mucopolysaccharides and other material on bio-persistent fibres in the lung. In addition to ferritin, the prevalent form of iron in asbestiform bodies, hematite is also present, and this suggests that there is an active process of alteration of iron chemistry within the asbestiform body. This mechanism can trigger fibre-related diseases, with potential DNA damage and resistance to apoptosis [30].

In FE-induced lesions, the Perls' staining showed the presence of ferruginous bodies that can react with the surrounding tissue by triggering a series of cellular reactions which attempt to re-establish a balance in the iron metabolism. Our results showed that following FE exposure, in most of the cases with fibre deposits, the

formation of asbestiform bodies of different shapes and sizes was observed, which covered either the entire fibre or part of it. In mesotheliomas, fibres were scarce but iron deposits were observed between the tumour cells, probably because fibres were incorporated by neoplastic cells and are no longer visible. Iron deposits or asbestiform bodies were stained in blue with Perls' and showed positivity for ferritin by IHC. Comparing the two methods developed, Perls' staining was found to be the most suitable for observing fibres in lung tissues.

Conclusion

In conclusion, this study confirmed that FE exposure promotes the onset of fibrotic lesions at pleural level, as fibrous plaques or nodules and fibrosis, through a mechanism similar to other form of asbestos. From a technical perspective, the Ashcroft analysis allowed the quantification of total fibrosis, whereas the IHC analysis gave information on the different stages of fibrosis formation, underlying the importance of both methods in the mechanistic studies of tissue fibrogenesis.

These results combined with the cluster of cases of lung fibrosis and the several cases of pleural plaques reported in Biancavilla residents [19], corroborate the need to promote health and epidemiological surveillance plans of respiratory diseases in population living in FE contaminated sites.

Supplementary Information

The online version contains supplementary material available at https://doi.org/10.1186/s12995-024-00434-5.

Supplementary Material 1.

Acknowledgements
We thank Dr. Morando Soffritti and Dr. Fiorella Belpoggi for their seminal contribution over the years to the RI in vivo long-term studies on fluoro-edenite.

Authors' contributions
ET, FG, DM contributed equally as first authors, performed and designed the study and produced the first draft of the manuscript. CB, AZ, LF and PC contributed to the design of the study, reviewed and edited the manuscript. All authors critically revised and approved the final manuscript.

Funding
The study was supported by the Italian National Institute for Insurance against Accidents at Work (INAIL) grant BRIC 2019 project under theme ID 55 "Development of tools for the updating of epidemiological surveillance methods and analytical research on asbestos-related diseases".

Availability of data and materials
Not applicable.

Data availability
No datasets were generated or analysed during the current study.

Declarations

Ethics approval and consent to participate
Not applicable.

Consent for publication
Not applicable.

Competing interests
The authors declare no competing interests.

Received: 19 April 2024 Accepted: 22 August 2024
Published: 27 December 2024

References

1. Di Paola M, Mastrantonio M, Carboni M, Belli S, Grignoli M, Comba P, Nesti M. Mortality from malignant pleural neoplasms in Italy in the years 1988–1992. Rapporti ISTISAN. 1996;96:1–30.
2. Paoletti L, Batisti D, Bruno C, Di Paola M, Gianfagna A, Mastrantonio M, Nesti M, Comba P. Unusually high incidence of malignant pleural mesothelioma in a town of eastern Sicily: an epidemiological and environmental study. Arch Environ Health. 2000;55:392–8.
3. Pasetto R, Bruni B, Bruno C, D'antona C, De Nardo P, Di Maria G, Di Stefano R, Fiorentini C, Gianfagna A, Marconi A. Problematiche sanitarie della fibra anfibolica di Biancavilla: aspetti epidemiologici, clinici e sperimentali. Not Ist Super Sanità. 2004;17:8–10.
4. Fazzo L, Comba P. The role of high risk groups in environmental health research. Ann Ist Super Sanita. 2004;40:417–26.
5. Cernigliaro A, Fano V, Addario SP, Caruso S, Pennisi P, Forastiere F, Perucci CA, Comba P, Scondotto S. Mortality and hospital discharges in the population of Biancavilla (Sicily) contaminated by natural fibres. Epidemiol Prev. 2006;30:227–31.
6. Putzu MG, Bruno C, Zona A, Massiccio M, Pasetto R, Piolatto PG, Comba P. Fluoro-edenitic fibres in the sputum of subjects from Biancavilla (Sicily): a pilot study. Environ Health. 2006;5:20.
7. Burragato F, Comba P, Baiocchi V, Palladino D, Simei S, Gianfagna A, Paoletti L, Pasetto R. Geo-volcanological, mineralogical and environmental aspects of quarry materials related to pleural neoplasm in the area of Biancavilla, Mount Etna (Eastern Sicily, Italy). Environ Geol. 2005;47:855–68.
8. Gianfagna A, Ballirano P, Bellatreccia F, Bruni B, Paoletti L, Oberti R. Characterization of amphibole fibres linked to mesothelioma in the area of Biancavilla, Eastern Sicily, Italy. Mineral Mag. 2003;67:1221–9.
9. Bruno C, Comba P, Zona A. Adverse health effects of fluoro-edenitic fibers: epidemiological evidence and public health priorities. Ann N Y Acad Sci. 2006;1076:778–83.
10. Comba P, Gianfagna A, Paoletti L. Pleural mesothelioma cases in Biancavilla are related to a new fluoro-edenite fibrous amphibole. Arch Environ Health. 2003;58:229–32. https://doi.org/10.3200/aeoh.58.4.229-232.
11. Mazziotti-Tagliani S, Andreozzi GB, Bruni BM, Gianfagna A, Pacella A, Paoletti L. Quantitative chemistry and compositional variability of fluorine fibrous amphiboles from Biancavilla (Sicily, Italy). Periodico di Mineralogia. 2009;78:65–74.
12. IARC. Some nanomaterials and some fibres. 2017. p. 111.
13. NIOSH. Asbestos fibers and other elongate mineral particles: State of the science and roadmap for research. Curr Intell Bull. 2011;62:1–153.
14. Gianfagna A, Oberti R. Fluoro-edenite from Biancavilla (Catania, Sicily, Italy): crystal chemistry of a new amphibole end-member. Am Miner. 2001;86:1489–93.
15. Soffritti M, Minardi F, Bua L, Degli Esposti D, Belpoggi F. First experimental evidence of peritoneal and pleural mesotheliomas induced by fluoro-edenite fibres present in Etnean volcanic material from Biancavilla (Sicily, Italy). Eur J Oncol. 2004;9:169–75.
16. Belpoggi F, Tibaldi E, Lauriola M, Bua L, Falcioni L, Chiozzotto D, Manservisi F, Manservigi M, Soffritti M. The efficacy of long-term bioassays in predicting human risks: mesotheliomas induced by fluoro-edenitic fibres

present in lava stone from the Etna volcano in Biancavilla, Italy. Eur J Oncol. 2011;16:185–95.
17. Conti S, Minelli G, Manno V, Iavarone I, Comba P, Scondotto S, Cernigliaro A. Health impact of the exposure to fibres with fluoro-edenitic composition on the residents in Biancavilla (Sicily, Italy): mortality and hospitalization from current data. Ann Ist Super Sanita. 2014;50:127–32.
18. Comba P, Fazzo L, Zona A. Respiratory illness in asbestos contaminated sites: the role of environmental exposure. Eur Respir J. 2011;38:248–50.
19. Bruno C, Di Stefano R, Ricceri V, La Rosa M, Cernigliaro A, Ciranni P, Di Maria G, Mandrioli D, Zona A, Comba P. Fluoro-edenite non-neoplastic diseases in Biancavilla (Sicily, Italy): pleural plaques and/or pneumoconiosis? Ann Ist Super Sanità. 2023;59:187–93.
20. Ashcroft T, Simpson JM, Timbrell V. Simple method of estimating severity of pulmonary fibrosis on a numerical scale. J Clin Pathol. 1988;41:467–70.
21. Hübner RH, Gitter W, Eddine El Mokhtari N, Mathiak M, Both M, Bolte H, Freitag-Wolf S, Bewig B. Standardized quantification of pulmonary fibrosis in histological samples. Biotechniques. 2008;44:507–17.
22 Robbe A, Tassin A, Carpentier J, Declèves A-E, MekindaNgono ZL, Nonclercq D, Legrand A. Intratracheal bleomycin aerosolization: the best route of administration for a scalable and homogeneous pulmonary fibrosis rat model? Biomed Res Int. 2015;2015:198418.
23. Sauter JL, Dacic S, Galateau-Salle F, Attanoos RL, Butnor KJ, Churg A, Husain AN, Kadota K, Khoor A, Nicholson AG. The 2021 WHO classification of tumors of the pleura: advances since the 2015 classification. J Thorac Oncol. 2022;17:608–22.
24 Ostrowska-Podhorodecka Z, Ding I, Norouzi M, McCulloch CA. Impact of vimentin on regulation of cell signaling and matrix remodeling. Front Cell Dev Biol. 2022;10:869069.
25. Cheng F, Shen Y, Mohanasundaram P, Lindström M, Ivaska J, Ny T, Eriksson JE. Vimentin coordinates fibroblast proliferation and keratinocyte differentiation in wound healing via TGF-β–Slug signaling. Proc Natl Acad Sci. 2016;113:E4320–7.
26. Challa AA, Stefanovic B. A novel role of vimentin filaments: binding and stabilization of collagen mRNAs. Mol Cell Biol. 2011;31:3773–89.
27. D'Urso M, Kurniawan NA. Mechanical and physical regulation of fibroblast–myofibroblast transition: from cellular mechanoresponse to tissue pathology. Front Bioeng Biotechnol. 2020;8:609653.
28. Ghio AJ, Churg A, Roggli VL. Ferruginous bodies: implications in the mechanism of fiber and particle toxicity. Toxicol Pathol. 2004;32:643–9.
29. Gandolfi NB, Gualtieri AF, Pollastri S, Tibaldi E, Belpoggi F. Assessment of asbestos body formation by high resolution FEG–SEM after exposure of Sprague-Dawley rats to chrysotile, crocidolite, or erionite. J Hazard Mater. 2016;306:95–104.
30. Pascolo L, Gianoncelli A, Schneider G, Salomé M, Schneider M, Calligaro C, Kiskinova M, Melato M, Rizzardi C. The interaction of asbestos and iron in lung tissue revealed by synchrotron-based scanning X-ray microscopy. Sci Rep. 2013;3:1123.

Publisher's Note